

Automatic Generation of Efficient Sparse Tensor Format Conversion Routines

Stephen Chou
MIT CSAIL
Cambridge, MA, USA
s3chou@csail.mit.edu

Fredrik Kjolstad
MIT CSAIL
Cambridge, MA, USA
fred@csail.mit.edu

Saman Amarasinghe
MIT CSAIL
Cambridge, MA, USA
saman@csail.mit.edu

Abstract

This paper shows how to generate code that efficiently converts sparse tensors between disparate storage formats (data layouts) like CSR, DIA, ELL, and many others. We decompose sparse tensor conversion into three logical phases: coordinate remapping, analysis, and assembly. We then develop a language that precisely describes how different formats group together and order a tensor’s nonzeros in memory. This enables a compiler to emit code that performs complex reorderings (remappings) of nonzeros when converting between formats. We additionally develop a query language that can extract complex statistics about sparse tensors, and we show how to emit efficient analysis code that computes such queries. Finally, we define an abstract interface that captures how data structures for storing a tensor can be efficiently assembled given specific statistics about the tensor. Disparate formats can implement this common interface, thus letting a compiler emit optimized sparse tensor conversion code for arbitrary combinations of a wide range of formats without hard-coding for any specific one.

Our evaluation shows that our technique generates sparse tensor conversion routines with performance between 0.99 and $2.2\times$ that of hand-optimized implementations in two widely used sparse linear algebra libraries, SPARSKIT and Intel MKL. By emitting code that avoids materializing temporaries, our technique also outperforms both libraries by between 1.4 and $3.4\times$ for CSC/COO to DIA/ELL conversion.

Keywords sparse tensor conversion, sparse tensor assembly, sparse tensor algebra, sparse tensor formats

1 Introduction

Sparse multidimensional arrays (tensors), which contain mostly zeros, are a convenient representation for data in many domains, including data analytics [2, 6] and machine learning [34, 39] among others. Countless formats for storing sparse tensors in memory have been proposed, many of which are used in real-world applications since no format is universally superior in every circumstance.

It is desirable for a general-purpose sparse tensor algebra library or framework to support efficiently converting tensors between as many combinations of formats as possible.

This is because applications typically need to perform different operations on the same tensor, and each operation may require the tensor to be stored in a distinct format for optimal performance. Importing data and transforming it to a sparse tensor, for instance, can be done efficiently if the tensor is constructed in the COO format, since COO supports efficient appends of new nonzeros. If all of the tensor’s nonzeros are clustered along a few dense diagonals though, then storing it in the DIA format reduces its memory footprint, since DIA only has to store each nonempty diagonal’s offset from the main diagonal. Thus, it would be more efficient to compute with the tensor in DIA as that reduces memory traffic. This requires first converting the tensor from COO to DIA.

Existing sparse linear and tensor algebra libraries, such as SPARSKIT [41] and Intel MKL [20], typically provide routines for converting sparse matrices and tensors between specific formats. Many libraries support a large number (N) of formats though, so it is impractical to hand-implement efficient conversion routines for all N^2 combinations of source and target formats. Instead, these libraries mostly only support direct conversions to and from some arbitrary canonical format (e.g., CSR for SPARSKIT). Thus, to convert a tensor from COO to DIA using SPARSKIT (or Intel MKL), an application must first convert the tensor to CSR and then once more to DIA. This doubles the number of conversions, which is suboptimal given that even efficiently converting a tensor once incurs significant overhead that must be amortized [14, 48]. Worse, this approach is not even an option if an application uses formats that are not supported at all by libraries. The developer must then hand-implement efficient custom conversion routines for each format, which are typically complicated and tedious to write and optimize. This motivates a technique that can instead automatically generate such format conversion routines.

1.1 Challenges

For many reasons, existing sparse tensor and linear algebra compilers such as taco [14, 24, 25] cannot generate efficient sparse tensor conversion routines for many formats.

Disparate orderings of nonzeros Different formats group together and order a tensor’s nonzeros in memory in distinct, potentially complex ways. CSR, for instances, stores nonzeros row by row, while DIA stores them diagonal by diagonal (Figure 1, center) and many other formats store nonzeros

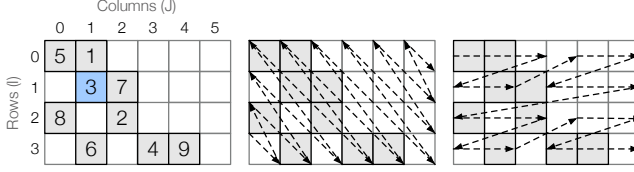


Figure 1. A sparse 4×6 tensor (matrix). Nonzeros can be ordered in memory not only by row or by column, but also by diagonal (center) or even by block (right).

in even more complex orderings like Morton order [12, 29]. This necessitates a language that can precisely describe all the ways in which different formats order nonzeros, so a compiler knows exactly how generated code needs to reorder a tensor’s nonzeros when converting between formats.

Reordering nonzeros Efficiently reordering a sparse tensor’s nonzeros is challenging when the source and target formats use compressed data structures, as these data structures restrict the order in which nonzeros can be efficiently iterated or inserted. CSR, for instance, uses an unpadded segmented vector that stores the segments (representing rows) and the nonzeros within each segment contiguously. This layout makes it inefficient to insert nonzeros in random order since, without knowing how many nonzeros will be in each row, each insertion requires shifting all stored nonzeros in subsequent rows. COO, however, can store nonzeros in any order but can only be efficiently iterated in that order, thus complicating conversions to CSR. One way to resolve such ordering inconsistencies is to simply explicitly sort the nonzeros into the target format’s ordering. However, this incurs significant overhead. So instead, many efficient conversion algorithms first compute statistics about the input tensor (e.g., number of nonzeros per row, bandwidth, etc.) and use those statistics to coordinate the reordering of nonzeros, eliminating the need to sort while minimizing data shuffling. Different target formats require distinct sets of statistics about the input tensor for efficient conversion. And depending on input tensor’s format, efficiently computing those statistics can require very different algorithms. To support conversion between arbitrary formats, a compiler needs to be able to generate efficient code to compute varied statistics about input tensors stored in arbitrary formats.

Disparate data structures Different tensor formats use disparate data structures to store nonzeros. Some explicitly store the coordinates of each nonzero, using data structures ranging from segmented vectors to linked lists to hash maps. Others use varying sets of parameters to implicitly encode sequences of coordinates of nonzeros. To support conversion between a wide range of formats, a compiler must be able to reason about how to insert nonzeros into all those different data structures in possibly arbitrary order, even if they do not necessarily support efficient random access.

1.2 Contributions

We propose a technique to generate efficient sparse tensor conversion routines for a wide range of disparate formats, building on recent work on sparse tensor algebra compilation [14, 24, 25]. We decompose a large class of tensor conversion algorithms into three logical phases (Section 3). Then, to facilitate generating code for each phase, we develop **coordinate remapping notation** that precisely describes how different tensor formats group together and order nonzeros in memory (Section 4), **attribute query language** that specifies what statistics about a tensor are needed in order to efficiently pack the tensor into different formats (Section 5), and a **tensor assembly abstract interface** that consists of functions to capture how results of attribute queries are used to efficiently assemble many kinds of sparse tensor data structures (Section 6).

As we will show, the conciseness of these abstractions makes it easy to provide specifications that describe how to efficiently construct sparse tensors in many formats. Our technique uses these specifications to emit code that efficiently packs a tensor’s nonzeros in arbitrary order into the desired target format. Combined with recent work that shows how to emit code for iterating tensors in the desired source format, our technique can then generate efficient sparse tensor conversion routines for arbitrary combinations of formats.

We have implemented a prototype of our technique in *taco*. Our evaluation shows that, for many combinations of source and target formats, our technique generates conversion routines with performance between 0.99 and 2.2× that of hand-optimized implementations in SPARSKIT and Intel MKL, two widely used sparse linear algebra library. Our technique also emits direct conversion routines that are not implemented in either library, which lets us further optimize tensor conversions from CSC and COO to DIA and ELL by between 1.4 and 3.4× (Section 7).

2 Background

There exist a wide variety of formats for storing sparse tensors in memory. Figure 2 shows four examples of commonly used sparse tensor formats; for an overview of additional formats that have been proposed, we refer readers to Chou et al. [14]. The COO format [7] represents a sparse tensor as a list of its nonzeros, storing the complete coordinates and value of each nonzero. COO supports efficiently appending new nonzeros, though it also wastes significant amounts of memory storing redundant row coordinates. The CSR format [45] compresses out the redundant row coordinates by grouping all nonzeros in the same row together and using a pos array to map nonzeros to each row. However, inserting a nonzero at some arbitrary coordinates into CSR is expensive as all nonzeros in subsequent rows have to be shifted in memory. The DIA [42] format stores nonzeros along the same

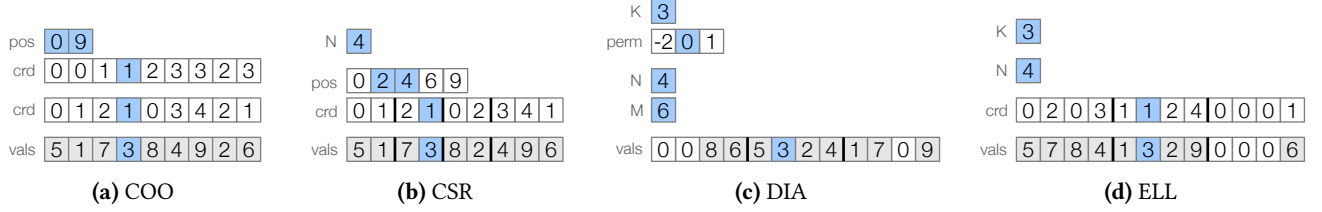


Figure 2. The same tensor as shown in Figure 1, stored in disparate sparse tensor formats.

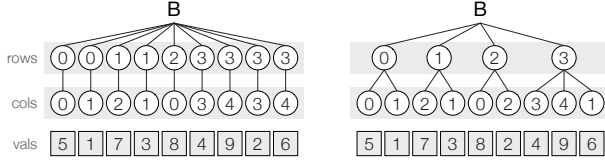


Figure 3. Coordinate hierarchy representations of the same tensor (Figure 1) stored in COO (left) and CSR (right).

diagonal together in memory, while the ELL [23] format stores the k -th nonzero of each row together. Such orderings of nonzeros expose vectorization opportunities for sparse matrix-vector multiplication [16] and can also further reduce memory footprint. However, DIA is only suitable for diagonal and banded matrices, while ELL is only suitable if numbers of nonzeros per row is bounded. As these examples show, there is no universally superior format for storing sparse matrices. The same is true for higher-order sparse tensors, for which even more formats have been proposed [8, 29, 30, 43] that use disparate data structures and ordering schemes to store nonzeros, each with distinct trade-offs.

2.1 Coordinate Hierarchy Abstraction

Chou et al. [14] describe how tensors stored in disparate formats can be represented as *coordinate hierarchies* that have varying structures but expose the same abstract interface. Figure 3 show examples of coordinate hierarchies that represent a matrix in different formats. Each stored component is represented by a path from the root to a leaf, with labels along the path denoting the component’s coordinates.

We can then decompose sparse tensor formats into *level formats* that each stores a coordinate hierarchy level, which represents a tensor dimension. CSR (Figure 2b), for instance, can be decomposed into two level formats, *dense* and *compressed*, that store the row and column levels respectively. The dense level format implicitly encodes all rows using just a parameter N to store the dimension’s size. By contrast, the compressed level format uses two arrays, *pos* and *crd*, to store column coordinates of nonzeros in each row. All level formats, however, expose the same static interface consisting of *level functions*, which describe how to access a format’s data structures, and *properties*, which describe characteristics of the data as stored (e.g., if nonzeros are stored in order).

Structured sparse tensor formats like DIA and ELL, which do not group nonzeros lexicographically by their coordinates, can also be decomposed into level formats by casting them as formats for tensors with additional dimensions. For example, a DIA matrix can be cast as a 3rd-order tensor where each slice contains only nonzeros that lie on the same diagonal; Figure 5 demonstrates one way in which this can be done. We can then decompose DIA into three level formats: one that stores the set of nonempty diagonals in a *perm* array of size K , another that encodes the set of rows in each diagonal, and a third that encodes the column coordinates of each nonzero. Such a decomposition lets a sparse tensor algebra compiler better reason about how tensors stored in DIA and similar structured formats can be efficiently iterated, which is crucial for generating fast tensor algebra code.

The coordinate hierarchy abstraction lets a compiler generate efficient code to iterate over sparse tensors in disparate formats by simply emitting code to traverse coordinate hierarchies. This entails recursively generating a set of nested loops that each iterates over a coordinate hierarchy level. The compiler generates each loop by emitting calls to level functions that describe how to efficiently access a level. Then, to obtain code that iterates over a tensor in any desired format, the level function calls are simply replaced with the desired format’s implementations of those level functions. This approach lets a compiler generate efficient code for disparate formats without hard-coding for any specific one.

3 Problem Formulation

Figure 4 shows three examples of sparse tensor conversion routines that efficiently convert tensors between different storage formats. As these examples illustrate, different combinations of source and target formats require vastly dissimilar code. All three routines perform distinct computations to determine how much memory to allocate for the output and where exactly to insert each of the input tensor’s nonzeros. In fact, they do not even iterate over the input nonzeros the same number of times; Figure 4b accesses each nonzero once, while the other two examples iterate over the input twice.

It turns out, however, that efficient algorithms for converting sparse tensors between a wide range of disparate formats can all be decomposed into three logical phases: *coordinate remapping*, *analysis*, and *assembly*. Figure 4 identifies these different phases using distinct background colors.

```

1 bool nonempty[2 * N - 1] = {0};
2 for (int i = 0; i < N; i++) {
3     for (int pA2 = A_pos[i];
4         pA2 < A_pos[i+1]; pA2++) {
5         int j = A_crd[pA2];
6         int k = j - i;
7         nonempty[k + N - 1] = true;
8     }
9 }
10 int* B_perm = new int[2 * N - 1];
11 int K = 0;
12 for (int i = -N + 1; i < N; i++) {
13     if (nonempty[i + N - 1])
14         B_perm[K++] = i;
15 }
16 double* B_vals = new double[K * N]();
17 int* B_rperm = new int[2 * N - 1];
18 for (int i = 0; i < K; i++) {
19     B_rperm[B_perm[i] + N - 1] = i;
20 }
21 for (int i = 0; i < N; i++) {
22     for (int pA2 = A_pos[i];
23         pA2 < A_pos[i+1]; pA2++) {
24         int j = A_crd[pA2];
25         int k = j - i;
26         int pB1 = B_rperm[k + N - 1];
27         int pB2 = pB1 * N + i;
28         B_vals[pB2] = A_vals[pA2];
29     }
30 }

```

(a) CSR to DIA

```

1 int K = 0;
2 for (int i = 0; i < N; i++) {
3     int ncols = A_pos[i+1] - A_pos[i];
4     K = max(K, ncols);
5 }
6 int* B_crd = new int[K * N]();
7 double* B_vals = new double[K * N]();
8 for (int i = 0; i < N; i++) {
9     int count = 0;
10    for (int pA2 = A_pos[i];
11        pA2 < A_pos[i+1]; pA2++) {
12        int j = A_crd[pA2];
13        int k = count++;
14        int pB2 = k * N + i;
15        B_crd[pB2] = j;
16        B_vals[pB2] = A_vals[pA2];
17    }
18 }

```

(b) CSR to ELL

```

1 int count[N] = {0};
2 for (int pA1 = A_pos[0];
3     pA1 < A_pos[1]; pA1++) {
4     int i = A1_crd[pA1];
5     count[i]++;
6 }
7 int* B_pos = new int[N + 1];
8 B_pos[0] = 0;
9 for (int i = 0; i < N; i++) {
10    B_pos[i + 1] = B_pos[i] + count[i];
11 }
12 int* B_crd = new int[pos[N]];
13 double* B_vals = new double[pos[N]];
14 for (int pA1 = A_pos[0];
15     pA1 < A_pos[1]; pA1++) {
16     int i = A1_crd[pA1];
17     int j = A2_crd[pA1];
18     int pB2 = pos[i]++;
19     B_crd[pB2] = j;
20     B_vals[pB2] = A_vals[pA2];
21 }
22 for (int i = 0; i < N; i++) {
23     B_pos[N - i] = B_pos[N - i - 1];
24 }
25 B_pos[0] = 0;

```

(c) COO to CSR

Figure 4. Code (in C++) to convert sparse matrices between different source and target formats. The background colors identify distinct logical phases of format conversion (green for coordinate remapping, yellow for analysis, and blue for assembly).

The coordinate remapping phase iterates over the input tensor and, for each nonzero, computes additional coordinates as functions of the nonzero’s original coordinates. What and how the additional coordinates are computed depend on the target format. For instance, code in Figure 4a, which converts a matrix to DIA, computes a new coordinate k as the difference between the column and row coordinates (lines 6 and 24). Coordinate remapping conceptually transforms the input tensor to a hypersparse higher-order tensor. The lexicographic coordinate ordering of nonzeros in the transformed (remapped) tensor reflects how nonzeros are laid out in the target format, as illustrated in Figure 5.

The analysis phase computes statistics about the input tensor that are later used to ensure sufficient memory is allocated for storing nonzeros in the target format. The exact statistics that are computed also depend on the target format. Figure 4a, for instance, computes the exact set of all nonempty diagonals in the input matrix (lines 1–8), with distinct diagonals identified by offsets (k) computed in the coordinate remapping phase. Figure 4b, by contrast, computes the maximum number of nonzeros in any row of the input matrix (lines 1–5), while Figure 4c computes the number of nonzeros in each row of the input matrix (lines 1–6).

Finally, the assembly phase iterates over the input tensor and inserts each nonzero into the output data structures. Again, where each nonzero is inserted ($pB2$) depends on the target format. Figure 4a computes $pB2$ as a function of each nonzero’s row coordinate and its offset k (as computed in the coordinate remapping phase), in such a way that nonzeros

with the same offset are grouped together in the output (lines 25–26). By contrast, Figure 4c simply appends each nonzero to its row’s corresponding segment in the `crd` array (line 19).

In the next three sections, we discuss how our technique generates efficient code to perform coordinate remapping (Section 4), analysis (Section 5), and assembly (Section 6). While each phase is logically distinct, our technique is able to emit code that fuses different phases if it is beneficial to do so. This lets us generate code like Figure 4a, which fuses coordinate remapping with both the analysis and assembly phases to avoid materializing the offsets of the nonzeros.

4 Coordinate Remapping

As explained in Section 3, the first phase of efficient sparse tensor conversion algorithms logically transforms (remaps) the input tensor to a higher-order one, such that the lexicographic coordinate ordering of nonzeros in the remapped tensor reflects how nonzeros are stored in the target format. We propose a new language called *coordinate remapping notation*, which precisely describes how a tensor can be remapped so as to capture the various ways that different tensor formats group and order nonzeros in memory. We further show how our technique generates code that applies a coordinate remapping to remap the input tensor as part of format conversion. This eliminates the need for end users to hand-implement additional code that separately performs such a remapping, which the technique of Chou et al. [14] requires for conversions to structured tensor formats.

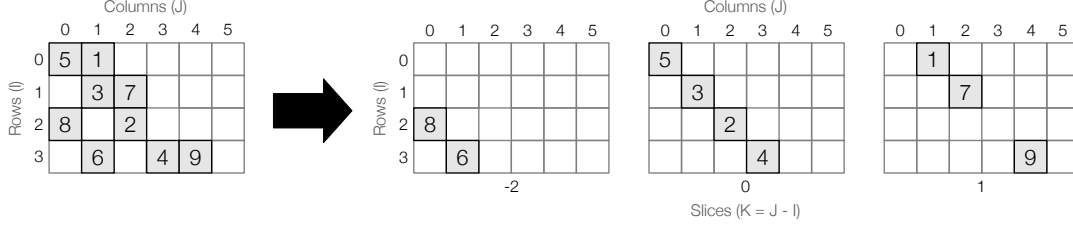


Figure 5. Applying the coordinate remapping $(i, j) \rightarrow (j-i, i, j)$ to a matrix transforms (remaps) it to a 3rd-order tensor where each slice contains all nonzeros that are on the same diagonal in the original matrix. The lexicographic coordinate ordering of nonzeros in the output exactly matches the order in which nonzeros are stored in DIA (Figure 2c).

```

remap_stmt := src_indices '->' dst_indices
src_indices := '(' ivar { ',' ivar } ')'
dst_indices := '(' ivar { ',' ivar } ')'
ivar_let := { var '=' ivar_expr 'in' } ivar_expr
ivar_expr := ivar_xor { '|' ivar_xor }
ivar_xor := ivar_and { '^' ivar_and }
ivar_and := ivar_shift { '&' ivar_shift }
ivar_shift := ivar_add { '<<' | '>>' } ivar_add
ivar_add := ivar_mul { '+' | '-' } ivar_mul
ivar_mul := ivar_factor { '*' | '/' | '%' } ivar_factor
ivar_factor := '(' ivar_expr ')' | ivar_counter | ivar | var | const
ivar_counter := '#' { ivar }

```

Figure 6. The syntax of coordinate remapping notation. Expressions in braces may be repeated any number of times.

4.1 Coordinate Remapping Notation

Figure 6 shows the syntax of coordinate remapping notation. Statements in coordinate remapping notation precisely specify how components in the input tensor map to components in a higher-order output tensor. For example, the statement

$$(i, j) \rightarrow (j-i, i, j)$$

maps every component A_{ij} of an input matrix to the corresponding component in the $(j-i)$ -th slice of the output tensor, which is three-dimensional. Applying this remapping to a matrix stored in any format transforms it to a 3rd-order tensor where each slice strictly contains all nonzeros that lie on the same diagonal in the original matrix. As illustrated in Figure 5, the lexicographic coordinate ordering of nonzeros in the resulting tensor thus accurately reflects the order in which nonzeros are stored in the DIA format.

Similarly, the BCSR format partitions a matrix into fixed-sized $M \times N$ blocks and stores components of each block contiguously in memory [19]. Such grouping of nonzeros can be expressed with the remapping

$$(i, j) \rightarrow (i/M, j/N, i, j),$$

which assigns components that lie within the same block to the same two-dimensional slice (identified by coordinates $(i/M, j/N)$) in the output tensor.

Coordinate remapping notation can express complex tensor reorderings. The following remapping, for instance, groups together nonzeros that lie within the same constant-sized

$N \times N \times N$ block and also orders the blocks as well as the nonzeros within each block in Morton order [32]:

$$\begin{aligned}
 (i, j, k) \rightarrow & \\
 (r=i/N \text{ in } s=j/N \text{ in } t=k/N \text{ in } & \\
 (r\&1) \mid ((s\&1)\<<1) \mid ((t\&1)\<<2) \dots, & i/N, j/N, k/N, \\
 r=i\%N \text{ in } s=j\%N \text{ in } t=k\%N \text{ in } & \\
 (r\&1) \mid ((s\&1)\<<1) \mid ((t\&1)\<<2) \dots, & i, j, k).
 \end{aligned}$$

The Morton code of each block and nonzero is computed by interleaving the bits of their coordinates using bitwise operations. This mapping exactly describes how the HiCOO tensor format orders nonzeros in memory [29].

Coordinate remapping notation also provides counters, denoted by the `"#"` symbol in Figure 6. Counters map nonzeros that share the same specified coordinates to distinct slices in the output tensor. For instance, the remapping

$$(i, j) \rightarrow (\#i, i, j)$$

assigns each nonzero that has the same i coordinate (i.e., that lies on the same row of the input matrix) to a distinct slice between the first and k -th slice in the output tensor, where k is the number of nonzeros in row i . This remapping effectively groups together (at most) one nonzero from each row in the matrix, which matches how formats like ELL and JAD [40] store nonzeros in memory.

4.2 Code Generation

In order to support generating sparse tensor conversion routines for arbitrary combinations of formats, we independently annotate each supported format with a coordinate remapping that describes how the format groups together and orders nonzeros. As the previous examples demonstrate, it is also simple for end users to add support for additional custom formats by using coordinate remapping notation to specify how the new formats lay out nonzeros in memory. Then, to support converting tensors between two specific formats, our technique emits code that iterates over the input tensor and transforms the coordinates of each nonzero by applying the target format's coordinate remapping.

To generate a set of nested loops that efficiently iterate over an input tensor in any source format, our technique uses the method Kjolstad et al. [25] proposed and Chou et al. [14] generalized, which we summarize at the end of Section 2.1.

Within the generated loops, our technique then emits code that computes each remapped nonzero’s additional coordinates as functions of the nonzero’s original coordinates, following the target format’s coordinate remapping.

To compute additional coordinates that are defined purely as arithmetic or bitwise expressions of the original coordinates, our technique simply inlines those expressions directly into the emitted code (e.g., lines 6 and 24 in Figure 4a, which compute the first coordinate in the output of the remapping $(i, j) \rightarrow (j-i, i, j)$). Remappings that contain let expressions are lowered by first emitting code to initialize the local variables and then inlining the expressions that use those local variables. For example, a remapped coordinate $r=i/N$ in $(r&1) \mid ((r&2)<<2)$ would be lowered to

```
int r = i/N;
int m = (r&1) \mid ((r&8)<<2);
```

Coordinate remappings that contain counters are lowered by emitting a set of counter variables for each distinct counter in the remapping. Each counter variable corresponds to a distinct set of coordinates (i_1, \dots, i_k) that can be used to index into the counter in the remapping, and the counter variable tracks how many input nonzeros with coordinates (i_1, \dots, i_k) have been iterated so far. Our technique additionally emits code that, for each nonzero with coordinates that correspond to counter variable c , first assigns the nonzero to the output tensor slice indexed by c and then increments c . So to apply the remapping $(i, j) \rightarrow (\#i, i, j)$ to a COO matrix, for instance, our technique emits the following code:

```
int counter[N] = {0}; // counter variables for #i
for (int p = 0; p < nnz; p++) {
  int i = A1_crd[p];
  int j = A2_crd[p];
  int k = counter[i]++; // k == #i
  // map A(i, j) to coordinates (k, i, j) ...
```

If the coordinates used to index into a counter are iterated in order though, our technique minimizes the number of counter variables in the generated code by having counter variables be reused across iterations. For instance, if the input matrix is instead stored in CSR, our technique infers from properties of the format (exposed through the abstraction discussed in Section 2.1) that we can efficiently iterate over nonzeros row by row. Thus, to apply the same coordinate remapping as before, our technique emits a single counter variable that is reused to remap each row. The result is optimized code shown on lines 8–13 in Figure 4b.

5 Attribute Queries

As we also saw in Section 3, to avoid having to constantly reallocate and shuffle around stored nonzeros, many efficient tensor conversion algorithms instead allocate memory in one shot based on some statistics about the input tensor. Computing these statistics, however, require very different

code depending on how the input tensor is stored. For instance, recall that to convert a matrix to ELL without having to dynamically resize the `crd` and `vals` arrays, one must first determine the maximum number of nonzeros K stored in any row of the input matrix. If the input matrix is stored in COO, then computing K requires constructing a histogram that records the number of nonzeros in each row, which in turn requires examining all the nonzeros in the matrix. If the input matrix is stored in CSR, however, then the number of nonzeros in each row can instead be directly computed from the `pos` array. Optimized code for converting CSR matrices to ELL thus does not need to make multiple passes over the input matrix’s nonzeros, reducing memory traffic.

We propose a new language called the *attribute query language* that precisely describes statistics of sparse tensors as aggregations over the coordinates of their nonzeros. The attribute query language is declarative, and attribute queries are specified independently of how the input tensor is actually stored. This lets our technique map attribute queries to equivalent sparse tensor computations and then simply leverage prior work on sparse tensor algebra compilation to generate optimized code for computing tensor statistics. As we show in Section 6, our technique can thus generate efficient tensor conversion routines while only requiring users to provide simple-to-specify attribute queries for each potential target format, as opposed to complicated loop nests for every combination of source and target formats.

5.1 Attribute Query Language

The attribute query language lets users compute summaries of a tensor’s sparsity structure by performing aggregations over the coordinates of the tensor’s nonzeros. All queries in the attribute query language take the form

```
select I1, ..., Im ->
  <aggr1> as label1, ..., <aggrn> as labeln
```

where each I_k denotes a dimension of a tensor A and $\langle \text{aggr}_k \rangle$ invokes the aggregation function `count`, `max`, `min`, or `id`.

For each subtensor A' of A with coordinates $(i_1, \dots, i_m) \in I_1 \times \dots \times I_m$, $\text{count}(I_k, \dots, I_l)$ computes the number of nonempty subtensors with distinct coordinates $(i_1, \dots, i_m, i_k, \dots, i_l) \in I_1 \times \dots \times I_m \times I_k \times \dots \times I_l$ that are contained in A' . For instance, if I, J, K represent the slice, row, and column dimensions of a 3rd-order tensor B , then the query

```
select I -> count(J) as nnr_in_slice
```

computes the number of nonempty rows contained in each slice of B , while the query

```
select I -> count(J, K) as nnz_in_slice
```

computes the number of nonzeros in each slice.

$\max(I_k)$ and $\min(I_k)$ compute, for each subtensor A' , the largest and smallest i_k such that the i_k -th slice of A' along dimension I_k is nonempty. For instance, if Q is the result of

```
select I ->
  min(J) as min_in_row, max(J) as max_in_row
```

applied to the matrix in Figure 1, then $Q[3].\text{min_in_row} == 1$ and $Q[3].\text{max_in_row} == 4$ since all nonzeros in row 3 (the last row) lie between columns 1 and 4.

Finally, `id` simply returns 1 if a subtensor A' contains nonzeros and 0 otherwise. So if R is the result of

```
select J -> id() as ne
```

again applied to the matrix in Figure 1, then $R[4].\text{ne} == 1$ since column 4 contains a nonzero while $R[5].\text{ne} == 0$ since the last column is empty.

The attribute query language can be used with coordinate remapping notation to compute even more complex attributes of structured tensors. For example, let A be a $K \times I \times J$ tensor obtained by applying the remapping $(i, j) \rightarrow (j-i, i, j)$ to a matrix B . Since each slice of A along dimension K corresponds to a unique diagonal in B , computing

```
select K -> id() as ne
```

on A results in a bit set that encodes the set of all nonempty diagonals in B . Furthermore, since the coordinate of each slice of A is defined to be the offset of the corresponding diagonal in B from the main diagonal, applying the query

```
select -> min(K) as lb, max(K) as ub
```

to A computes the lower and upper bandwidths of B .

5.2 Code Generation

To generate efficient code that computes an attribute query, our technique reformulates the query as sparse tensor algebra computation. The query is first lowered to a canonical form expressed in a variant of concrete index notation [24], which is a language for specifying tensor operations. The canonical form of the query then subsequently optimized by applying a set of transformations we define that simplify the computation. Finally, the optimized query in concrete index notation is compiled to imperative code by straightforwardly leveraging the techniques of Kjolstad et al. and Chou et al. [14, 24, 25], which take concrete index notation and generate efficient sparse tensor algebra kernels for operands in disparate formats. This approach works as long as query results are stored in a format like dense arrays that can itself be efficiently assembled without requiring attribute queries.

More precisely, let A be an $I_1 \times \dots \times I_r$ tensor obtained by applying some remapping to a $J_1 \times \dots \times J_n$ tensor B . Then, to compute an attribute query of the form

```
select I_1, ..., I_m -> id() as Q,
```

which invoke the `id` function, on A , our technique lowers the query to its canonical form in concrete index notation as

$$\forall_{j_1} \dots \forall_{j_n} Q_{i_1 \dots i_m} \mid = \text{map}(B_{j_1 \dots j_n}, 1).$$

The computation above logically iterates over every component of B , computes the coordinates (i_1, \dots, i_m) of each component $B_{j_1 \dots j_n}$ in the remapped tensor A , and sets the

corresponding component in the Boolean result tensor Q to true (1). The map operator returns the second argument if the first argument is nonzero (or true) and zero otherwise, which ensures only the nonzeros in B are aggregated. So if, for instance, C is a $K \times I \times J$ tensor obtained by applying the remapping $(i, j) \rightarrow (j-i, i, j)$ to a matrix D , then to compute `select K -> id() as Q` on C , our technique lowers the query to the computation $\forall_i \forall_j Q_{j-i} \mid = \text{map}(D_{ij}, 1)$. For each and only the nonzeros of D , this computation computes the nonzero's offset from the main diagonal and sets the corresponding component in Q to true. The query result Q thus strictly encodes the set of diagonals in D that have nonzeros.

In a similar way, our technique lowers count queries

```
select I_1, ..., I_m -> count(I_k, ..., I_l) as Q
```

on A to their canonical form

$$\begin{aligned} &(\forall_{i_1} \dots \forall_{i_l} Q_{i_1 \dots i_m} \mid = \text{map}(W_{i_1 \dots i_l}, 1)) \textbf{ where} \\ &(\forall_{j_1} \dots \forall_{j_n} W_{i_1 \dots i_m i_k \dots i_l} \mid = \text{map}(B_{j_1 \dots j_n}, 1)). \end{aligned}$$

The computation above first iterates over the nonzeros of B to compute the intermediate result W , which encodes whether each subtensor of A with coordinates $(i_1, \dots, i_m, i_k, \dots, i_l)$ is nonempty. The computation then sums over dimensions I_k to I_l of W in order to compute the number of aforementioned subtensors that are nonempty and contained in each higher-order subtensor with coordinates (i_1, \dots, i_m) .

Our technique also generates code for `max` queries

```
select I_1, ..., I_m -> max(I_k) as Q
```

by lowering them to their canonical form

$$\forall_{j_1} \dots \forall_{j_n} Q'_{i_1 \dots i_m} \text{ max} = \text{map}(B_{j_1 \dots j_n}, i_k - s + 1),$$

where s denotes the smallest possible coordinate along dimension I_k . The result is assumed to be initialized to the zero matrix, so by mapping each input tensor component to its remapped coordinate i_k plus the constant $(1 - s)$, we ensure that only the coordinates of nonzeros are actually aggregated. Q' can thus be interpreted as the actual result of the original query (i.e., Q) but just shifted by $(1 - s)$; in other words, $Q_{i_1 \dots i_m} \equiv Q'_{i_1 \dots i_m} + s - 1$. Similarly, `min` queries

```
select I_1, ..., I_m -> min(I_k) as Q
```

are lowered to their canonical form

$$\forall_{j_1} \dots \forall_{j_n} Q'_{i_1 \dots i_m} \text{ max} = \text{map}(B_{j_1 \dots j_n}, -i_k + t),$$

where t denotes one plus the largest possible coordinate along dimension I_k and Q' is the query result but negated and shifted by t ; in other words, $Q_{i_1 \dots i_m} \equiv -Q'_{i_1 \dots i_m} + t$.

After an attribute query is lowered to its canonical form, our technique eagerly applies a set of predefined transformations on the query computation in order to optimize its performance. Table 1 shows a subset of transformations that our technique uses. In general, these transformations exploit properties of the input tensor and its underlying storage format in order to reduce the number of dimensions that have to be iterated and to eliminate redundant temporaries.

Table 1. Example transformations that our technique applies to optimize attribute queries. We augment level formats with a property that specifies if a dimension stores explicit zeros, which lets our technique determine if a tensor stores only nonzeros.

Transformation	Definition	Preconditions and Postconditions
reduction-to-assign	$(\forall_{j_1} \dots \forall_{j_n} A_{i_1 \dots i_m} \oplus = \text{expr})$ $\implies (\forall_{j_1} \dots \forall_{j_n} A_{i_1 \dots i_m} = \text{expr})$	For each j_k , there exists an i_l such that $j_k \equiv i_l$. \oplus is any reduction operator.
inline-temporary	$(\forall_{i_1} \dots \forall_{i_m} A_{i_1 \dots i_l} \oplus = f(W_{i_1 \dots i_m}))$ where $(\forall_{j_1} \dots \forall_{j_n} W_{i_1 \dots i_m} = \text{expr})$ $\implies (\forall_{j_1} \dots \forall_{j_n} A_{i_1 \dots i_l} \oplus = f(\text{expr}))$	f is any function that takes only W as tensor operand. \oplus is any reduction operator or a simple assignment.
simplify-width-count	$(\forall_{j_1} \dots \forall_{j_n} A_{i_1 \dots i_m} += \text{map}(B_{j_1 \dots j_n}, c))$ $\implies (\forall_{j_1} \dots \forall_{j_{n-1}} A_{i_1 \dots i_m} += B'_{j_1 \dots j_{n-1}} \cdot c)$	B stores only nonzeros, and j_n is reduction variable that indexes into the innermost dimension of B (J_n). c is any constant. B' is a tensor that encodes the number of nonzeros in each slice of B ; the values of B' are not materialized but dynamically computed from level functions that define iteration over dimension J_n of B .
counter-to-histogram	$(\forall_{j_1} \dots \forall_{j_n} A_{i_1 \dots i_m} \text{max} = \text{map}(B_{j_1 \dots j_n}, \#j_k \dots j_l + 1))$ $\implies (\forall_{i_1} \dots \forall_{i_l} A_{i_1 \dots i_m} \text{max} = W_{i_1 \dots i_l})$ where $(\forall_{j_1} \dots \forall_{j_n} W_{i_1 \dots i_m j_k \dots j_l} += \text{map}(B_{j_1 \dots j_n}, 1))$	None.

To see how our technique optimizes attribute queries, consider the example query `select I -> count(J) as Q` applied to an $I \times J$ matrix B . As described before, our technique first lowers this query to its canonical form

$$(\forall_i \forall_j Q_i += \text{map}(W_{ij}, 1)) \text{ where } (\forall_i \forall_j W_{ij} = \text{map}(B_{ij}, 1)).$$

Our technique then proceeds to iteratively and eagerly apply the transformations shown in Table 1 on the computation above. In particular, each iteration variable bound to a \forall is used to independently index into a dimension of W , so the sub-statement that defines W satisfies the preconditions of the reduction-to-assign transformation. Our technique thus applies the aforementioned transformation on the substatement that defines W to get

$$(\forall_i \forall_j Q_i += \text{map}(W_{ij}, 1)) \text{ where } (\forall_i \forall_j W_{ij} = \text{map}(B_{ij}, 1)).$$

Then, since the temporary W is no longer the result of a reduction operation, our technique eliminates it by applying the inline-temporary transformation to get

$$\forall_i \forall_j Q_i += \text{map}(\text{map}(B_{ij}, 1), 1),$$

which is then trivially rewritten to $\forall_i \forall_j Q_i += \text{map}(B_{ij}, 1)$ by applying constant folding. If B is stored in COO, then we can directly apply the techniques of Kjolstad et al. and Chou et al. to lower this rewritten statement down to imperative code shown on lines 1–6 in Figure 4c. However, if B is stored in CSR without explicit zeros, then our technique additionally applies the simplify-width-count transformation followed by reduction-to-assign again to get the final query

$$\forall_i Q_i = B'_i,$$

where each component of B' is dynamically computed as `pos[i+1] - pos[i]`. The optimized query thus avoids iterating over B 's nonzeros, thereby reducing memory traffic.

6 Sparse Tensor Assembly

As explained in Section 2.1, a sparse tensor can be modeled as a hierarchical structure of coordinates, where each stored component is represented by a path from the root to a leaf. We can thus view any tensor format simply as a composition of level formats that each stores a level of a coordinate hierarchy. This abstraction lets us reason about sparse tensor assembly as coordinate hierarchy construction.

We extend the coordinate hierarchy abstraction with new primitives (level functions) that describe how each level can be efficiently constructed (assembled). These new level functions, unlike analogous ones that Chou et al. [14] propose, describe how coordinates and edges can be efficiently inserted into a coordinate hierarchy assuming certain statistics about the input tensor have been precomputed.

Figure 7 show how level formats that use disparate data structures to store a coordinate hierarchy level can implement the new assembly level functions. All these implementations expose the same static interface, which lets our code generator reason about and emit efficient code to convert tensors between a wide range of formats. And by using the same level formats to express different tensor formats that share common data structures, our technique can also reuse the same level function implementations to generate conversion routines for many different target formats. For example, the column dimensions of CSR tensors and the row dimensions of COO tensors can both be stored using the same level format (i.e., *compressed*). Our technique can thus use the same implementations of the new assembly level functions (for the compressed level format) to generate (portions of) code that convert tensors to either CSR or COO. This

limits the one-time effort needed to implement our extended coordinate hierarchy abstraction.

6.1 Assembly Abstraction

Our extended coordinate hierarchy abstraction assumes that coordinate hierarchies can be constructed level by level from top to bottom. The assembly of each level is decomposed into two logical phases: *edge insertion* and *coordinate insertion*.

The edge insertion phase, which is optional, logically bulk inserts edges into a coordinate hierarchy, connecting coordinates in one level to coordinates in the preceding parent level. Edge insertion models the assembly of data structures that map nonzeros to their containing subtensors. Depending on whether each position (i.e., node) in the parent level can be iterated in sequence, edge insertion can be done in a *sequenced* or *unsequenced* fashion.

Unsequenced edge insertion is defined in terms of three level functions that any level format may implement:

- `unseq_init_edges(szk-1, Qk) -> void`
- `unseq_insert_edges(pk-1, i1, ..., ik-1, qk) -> void`
- `unseq_finalize_edges(szk-1) -> void`

Q_k denotes the (complete) results of attribute queries that a level format specifies must be precomputed, while q_k denotes only the elements of Q_k indexed by coordinates (i_1, \dots, i_{k-1}) . sz_{k-1} is the size of the parent level and can be computed as a function of its own parent's size by calling the level function

`get_size(szk-1) -> szk,`

which all level formats must also implement. `unseq_init_edges` initializes data structures that the level format uses to logically store edges. Then, for each position p_{k-1} in the parent level, which represents a subtensor with coordinates (i_1, \dots, i_{k-1}) , `unseq_insert_edges` allocates some number of child coordinates to be connected to p_{k-1} . The number of child coordinates allocated can be computed as any function of q_k . Finally, `unseq_finalize_edges` inserts edges into the coordinate hierarchy such that each coordinate in the parent level is connected to as many children as it was previously allocated. Figure 8 (left) shows how these level functions can logically be invoked to bulk insert edges.

Sequenced edge insertion, by contrast, is defined in terms of just two level functions:

- `seq_init_edges(szk-1, Qk) -> void`
- `seq_insert_edges(pk-1, i1, ..., ik-1, qk) -> void`

These level functions are analogous to `unseq_init_edges` and `unseq_insert_edges` and can be invoked in similar ways. Sequenced edge insertion, however, assumes that all positions in the parent level are iterated in order. Thus, `seq_insert_edges` is responsible for both allocating the appropriate number of child coordinates to each parent and actually inserting the edges, and a separate `finalize` function is not necessary.

The coordinate insertion phase logically iterates over the input tensor's nonzeros and inserts their coordinates into

a coordinate hierarchy. Coordinate insertion models the assembly of data structures that store the actual coordinates and values of the nonzeros. This phase is defined in terms of the following level functions:

- `init_coords(szk-1, Qk) -> void`
- `init_{get|yield}_pos(szk-1) -> void`
- `{get|yield}_pos(pk-1, i1, ..., ik) -> pk`
- `insert_coord(pk-1, pk, i1, ..., ik) -> void`
- `finalize_{get|yield}_pos(szk-1) -> void`

`init_coords` allocates and initializes data structures for storing coordinates in a coordinate hierarchy level. If a level format implicitly encodes coordinates (e.g., as a fixed range) using some fixed set of parameters, then `init_coords` also compute those parameters as functions of the attribute query results Q_k . On the other hand, if a level format explicitly stores coordinates in memory, then the coordinates of nonzeros are inserted by invoking `insert_coord` for each nonzero. The position p_k at which each nonzero should be inserted is computed by invoking either `get_pos` or `yield_pos`. The former guarantees that nonzeros with the same coordinates are inserted at the same position. The latter allows duplicate coordinates to be inserted at different positions. Both functions, however, may rely on auxiliary data structures to track where to insert coordinates; `init_{get|yield}_pos` and `finalize_{get|yield}_pos` initializes and cleans up those data structures. Figure 8 (right) shows how all these level functions can be invoked to perform coordinate insertion.

6.2 Code Generation

To generate code that converts sparse tensors between two formats, our code generator emits loops that iterate over a tensor in the source format and apply the target format's coordinate remapping to each nonzero. This is done by applying the technique described in Section 4.2. Then, within each loop nest that iterates over the (remapped) input tensor, the code generator emits code that invokes the level functions described in Section 6.1 to store each nonzero into the result. The emitted code is finally specialized to the target format by inlining its implementations of the aforementioned level functions (e.g., as shown in Figure 7). This approach enables the code generator to support disparate target (and source) formats. At the same time, it limits the complexity of the code generator, since the code generator does not need to hard-code for specific data structures but can simply reason about how to invoke a fixed set of level functions.

To minimize memory traffic at runtime, our technique generates code that, wherever possible, fuses the assembly of adjacent levels in the result coordinate hierarchy. Adjacent levels can be assembled together as long as only the parent level requires a separate edge insertion phase (or if none do). As an example, none of the level formats that compose DIA requires edge insertion. Thus, our technique will emit code

<pre> unseq_init_edges(szk-1, Qk): pos = calloc(szk-1 + 1, int); seq_init_edges(szk-1, Qk): pos = malloc(szk-1 + 1, int); pos[0] = 0; yield_pos(pk-1, i1, ..., ik): return pos[pk-1]++; insert_coord(pk-1, pk, i1, ..., ik): crd[pk] = ik; init_coords(szk-1, Qk): perm = malloc(Nk - Mk, int); K = 0; for (i = Mk; i < Nk; i++) { if (Qk[0][i].ne) perm[K++] = i; } init_coords(szk-1, Qk): crd = calloc(szk-1, int); </pre>	<pre> unseq_insert_edges(pk-1, i1, ..., ik-1, qk): pos[pk-1 + 1] = qk[0].nir; seq_insert_edges(pk-1, i1, ..., ik-1, qk): pos[pk-1 + 1] = pos[pk-1] + qk[0].nir; finalize_yield_pos(szk-1): for (i = 0; i < szk-1; i++) pos[szk-1 - i] = pos[szk-1 - i - 1]; pos[0] = 0; get_size(szk-1): return pos[szk-1]; init_get_pos(szk-1): rperm = malloc(Nk - Mk, int); for (i = 0; i < K; i++) rperm[perm[i] - Mk] = i; get_size(szk-1): return szk-1 * K; insert_coord(pk-1, pk, i1, ..., ik): crd[pk] = ik; </pre>	<pre> unseq_finalize_edges(szk-1): prefix_sum(pos, szk-1 + 1); init_yield_pos(szk-1): pass; init_coords(szk-1, Qk): crd = malloc(pos[szk-1]), int); Qk := {select I1, ..., Ik-1 -> count(Ik) as nir} get_pos(pk-1, i1, ..., ik): return pk-1 * K + rperm[ik - Mk]; finalize_get_pos(szk-1): free(rperm); Qk := {select Ik -> 1 as ne} get_pos(pk-1, i1, ..., ik): return pk-1; get_size(szk-1): return szk-1; </pre>
----------------------------------------------------------------------------------------------------------------------------------------------------------------------------------------------------------------------------------------------------------------------------------------------------------------------------------------------------------------------------------------------------------------------------------------------------------------	----------------------------------------------------------------------------------------------------------------------------------------------------------------------------------------------------------------------------------------------------------------------------------------------------------------------------------------------------------------------------------------------------------------------------------------------------------------------------------------------------------------------------------------------	------------------------------------------------------------------------------------------------------------------------------------------------------------------------------------------------------------------------------------------------------------------------------------------------------------------------------------------------------------------------------------------------------------------------------------------

Figure 7. Implementations of the assembly abstraction, including definitions of level functions and the required attribute queries, for three different level formats: *compressed* (top), *squeezed* (middle), and *singleton* (bottom). The compressed level format stores the column dimension of CSR tensors as well as the row dimension of COO tensors. The squeezed level format stores the dimension of offsets in DIA tensors, while the singleton level format stores the column dimensions of COO and ELL tensors. M_k and N_k denote the lower and upper bounds of the k -th dimension respectively.

<pre> szk-1 = get_sizek-1(get_sizek-2(...(1)...)); unseq_init_edges(szk-1, Qk); for (position pk-1 in parent level ∃ coords i1, ..., ik-1 connecting pk-1 to root) { qk[:] = Qk[:][i1, ..., ik-1]; unseq_insert_edges(pk-1, i1, ..., ik-1, qk); } unseq_finalize_edges(szk-1); </pre>	<pre> init_coords(szk-1, Q); init_{get yield}_pos(szk-1); for (nonzero with coords i1, ..., ik) { for (j = 1; j <= k; j++) // can be unrolled pj = {get yield}_posj(pj-1, i1, ..., ij); insert_coord(pk-1, pk, i1, ..., ik); } finalize_{get yield}_pos(szk-1); </pre>
-------------------------------------------------------------------------------------------------------------------------------------------------------------------------------------------------------------------------------------------------------------------------------------------------	-----------------------------------------------------------------------------------------------------------------------------------------------------------------------------------------------------------------------------------------------------------------------------------

Figure 8. Unsequenced edge insertion (left) and coordinate insertion (right), expressed in terms of calls to level functions.

to convert any matrix to DIA by iterating over the matrix just once and assembling all output dimensions (levels) together.

For each set of levels that can be assembled together, our technique then simply has to emit code like shown in Figure 8 to perform edge insertion (if required) followed by coordinate insertion. If a level format implements both variants of edge insertion, then our technique selects one based on whether the parent level can be iterated in order. The code generator infers this from properties exposed through the coordinate hierarchy abstraction that specify if the parent level stores coordinates in order. If a level format implements `yield_pos` but does not permit storing duplicates of the same coordinate, then our technique also emits logic to perform deduplication on the fly by keeping track of inserted coordinates.

To see how our technique works, assume we are generating code to convert COO tensors to CSR. To obtain code that

assembles the column dimension of the result, the code generator first emits sequenced edge insertion code that has the same structure as Figure 8 (left), except with all level functions replaced by their sequenced counterparts. The emitted code is then specialized to CSR by replacing the level function calls with the compressed level format’s implementations of those functions (Figure 7, top). The result is lines 7–11 in Figure 4c, which iterate over all rows of the output in order and reserve exactly enough space to store each row’s nonzeros. In a similar way, the code generator emits code in Figure 8 (right) to perform coordinate insertion and then specializes it to CSR, yielding lines 12–25 in Figure 4c.

7 Evaluation

We evaluate our technique and find that it generates efficient sparse tensor conversion routines for many combinations

Table 2. Statistics about matrices used in our experiments.

#	Matrix	Domain	Dimensions	Nonzeros	Density	Symmetric	Nonempty Diagonals	Maximum Nonzeros/row
1	pdb1HYS	Protein data base	36K × 36K	4,344,765	3×10^{-3}	Yes	25,577	204
2	jnlbrng1	Optimization	40K × 40K	199,200	1×10^{-4}	Yes	5	5
3	obstclae	Optimization	40K × 40K	197,608	1×10^{-4}	Yes	5	5
4	chem_master1	Chemical master equation	40K × 40K	201,201	1×10^{-4}	No	5	5
5	rma10	3D CFD	46K × 46K	2,374,001	1×10^{-3}	No	17,367	145
6	dixmaanl	Optimization	60K × 60K	299,998	8×10^{-5}	Yes	7	5
7	cant	FEM/Cantilever	62K × 62K	4,007,383	1×10^{-3}	Yes	99	78
8	shyy161	CFD/Navier-Stokes	76K × 76K	329,762	6×10^{-5}	No	7	6
9	consph	FEM/Spheres	83K × 83K	6,010,480	9×10^{-4}	Yes	13,497	81
10	denormal	Counter-example problem	89K × 89K	1,156,224	1×10^{-4}	Yes	13	13
11	Baumann	Chemical master equation	112K × 112K	748,331	6×10^{-5}	No	7	7
12	cop20k_A	FEM/Accelerator	121K × 121K	2,624,331	2×10^{-4}	Yes	221,205	81
13	shipsec1	FEM	141K × 141K	3,568,176	2×10^{-4}	Yes	10,475	102
14	majorbasis	Optimization	160K × 160K	1,750,416	7×10^{-5}	No	22	11
15	scircuit	Circuit	171K × 171K	958,936	3×10^{-5}	No	159,419	353
16	mac_econ_fwd500	Economics	207K × 207K	1,273,389	9×10^{-5}	No	511	44
17	pwtkt	Wind tunnel	218K × 218K	11,524,432	2×10^{-4}	Yes	19,929	180
18	Lin	Structural problem	256K × 256K	1,766,400	3×10^{-5}	Yes	7	7
19	ecology1	Animal movement	1M × 1M	4,996,000	5×10^{-6}	Yes	5	5
20	webbase_1M	Web connectivity	1M × 1M	3,105,536	3×10^{-6}	No	564,259	4700
21	atmosmodd	Atmospheric model	1.3M × 1.3M	8,814,880	5×10^{-6}	No	7	7

of disparate source and target formats. The generated conversion routines have performance similar to or better than equivalent hand-implemented versions. We also find that, for combinations of source and target formats that are not directly supported by a library, our technique can further optimize conversions between those formats by emitting code that avoids materializing temporaries.

7.1 Experimental Setup

We implemented a prototype of our technique as extensions to the open-source taco tensor algebra compiler [25]. To evaluate it, we compare code that our technique generates against hand-implemented versions in SPARSKIT [41], a widely used [21, 35] Fortran sparse linear algebra library, and Intel MKL [20], a C and Fortran math processing library that is optimized for Intel processors. We also evaluate our technique against taco without our extensions.

All experiments are conducted on a 2.5 GHz Intel Xeon E5-2680 v3 machine with 30 MB of L3 cache and 128 GB of main memory. The machine runs Ubuntu 18.04.3 LTS. We compile code that our technique generates using GCC 7.4.0 and build SPARSKIT from source using GFortran 7.4.0. We run each experiment 100 times under cold cache conditions and report minimum serial execution times.

We run our experiments with real-world matrices of varying sizes and structures as inputs. These matrices, listed in Table 2, come from applications in disparate domains and are obtained from the SuiteSparse Matrix Collection [15].

7.2 Performance Evaluation

We measure the performance of sparse tensor conversion routines that our technique generates for seven distinct combinations of source and target formats:

- COO to CSR (coo_csr)
- COO to DIA (coo_dia)
- CSR to CSC (csr_csc)
- CSR to DIA (csr_dia)
- CSR to ELL (csr_ell)
- CSC to DIA (csc_dia)
- CSC to ELL (csc_ell)

where inputs and outputs in COO, CSR, or CSC are not assumed to be sorted (though nonzeros are still necessarily grouped by row/column in CSR/CSC). For each combination of formats, we also measure the performance of converting between those formats using SPARSKIT and Intel MKL. Both libraries implement routines that directly convert matrices from COO to CSR, CSR to CSC, and CSR to DIA. Additionally, SPARSKIT supports directly converting matrices from CSR to ELL. However, neither SPARSKIT nor Intel MKL implements routines that directly convert matrices between the remaining combinations of formats. Thus, to perform those conversions for non-symmetric matrices using either library, we first convert the input from its source format to a temporary in CSR and then convert the temporary from CSR to the desired target format. (If the input matrix is symmetric, however, then conversions from CSC to DIA/ELL can simply be cast as conversions from CSR to DIA/ELL.)

Figures 9 to 12 show the results of our experiments. As these results demonstrate, our technique outperforms or is comparable to SPARSKIT and Intel MKL on average for all

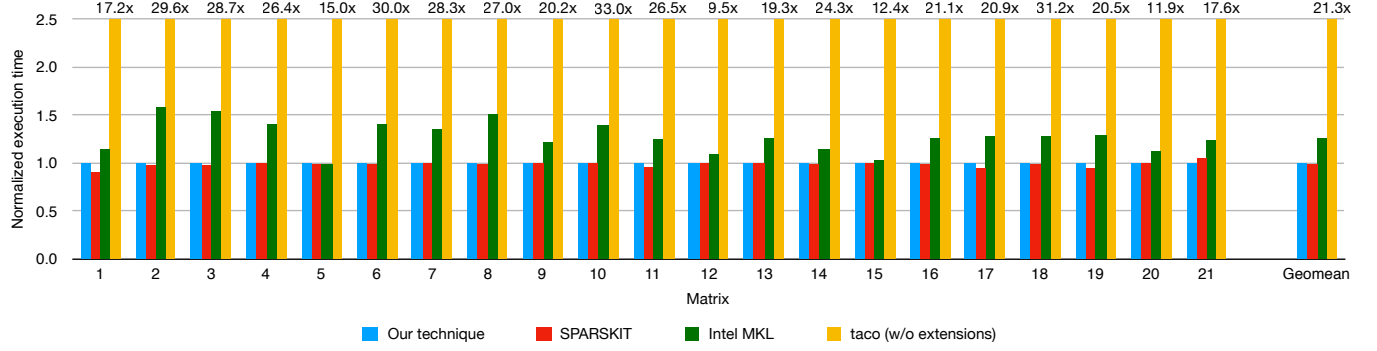


Figure 9. Normalized execution times of COO to CSR conversion (`coo_csr`), using code that our technique generates and other existing libraries as well as taco without our extensions. Results are normalized to that of our technique for each test matrix.

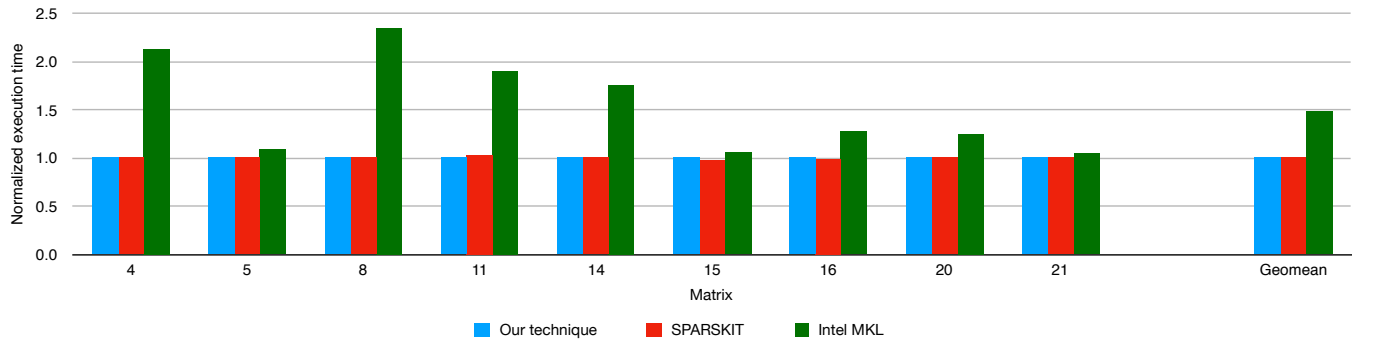


Figure 10. Normalized execution times of CSR to CSC conversion (`csr_csc`), using code that our technique generates and other existing libraries. Results are normalized to that of our technique for each test matrix. We only show results for nonsymmetric matrices, since CSR and CSC are equivalent for symmetric matrices.

combinations of source and target formats that we evaluate. On the whole, code that our technique emits to convert matrices from COO to CSR (`coo_csr`) and from CSR to CSC (`csr_csc`) exhibit similar performance as hand-implemented routines in SPARKIT and somewhat better performance than Intel MKL. This is unsurprising since our technique generates code that implement the same algorithms (variations of Gustavson’s HALFPERM algorithm [18]) as SPARKIT. Our technique also emits code to perform CSR to DIA conversion that is 2.2× faster than SPARKIT and 1.6× faster than Intel MKL on average. SPARKIT’s implementation of `csr_dia` supports extracting a bounded number (K) of nonempty diagonals from an $N \times N$ input matrix and storing them in the output. However, SPARKIT implements this capability inefficiently by performing the first K iterations of selection sort on the set of all $2N - 1$ diagonals, in order to identify and extract the densest diagonals. This incurs overhead of $(2K - 1)N$ memory accesses, which is significant if the input matrix only has K nonempty diagonals and $\sim KN$ nonzeros that must be copied to begin with. Furthermore, code that our technique emits to perform CSR to ELL conversion is 1.2× faster than SPARKIT on average. This is because our technique emits code that invokes `calloc` to

both allocate and zero-initialize the output arrays, whereas SPARKIT’s `csr_ell` kernel takes user-allocated output arrays as arguments and separately initializes those arrays.

Our technique also significantly outperforms SPARKIT by 3.4× on average for COO to DIA conversion, 2.6× for CSC to DIA conversion, and 1.4× for CSC to ELL conversion. Similarly, code that our technique emits outperforms Intel MKL by 3.2× for COO to DIA conversion and 2.2× for CSC to DIA conversion. As mentioned before, neither SPARKIT nor Intel MKL implements routines to directly convert between any of those combinations of formats. Thus, when the input is nonsymmetric or stored in COO, both libraries must incur additional memory accesses to construct temporary CSR matrices and then iterate over those temporaries again in order to perform the actual conversion to DIA or ELL. By contrast, our technique emits code that directly converts matrices from COO/CSC to DIA/ELL without materializing any temporary. This minimizes memory traffic and lets our technique achieve even greater speedups over SPARKIT and Intel MKL than we observe for CSR to DIA/ELL conversions, which the libraries directly implement.

Finally, we measure and compare against the performance of taco without our extensions for COO to CSR conversion.

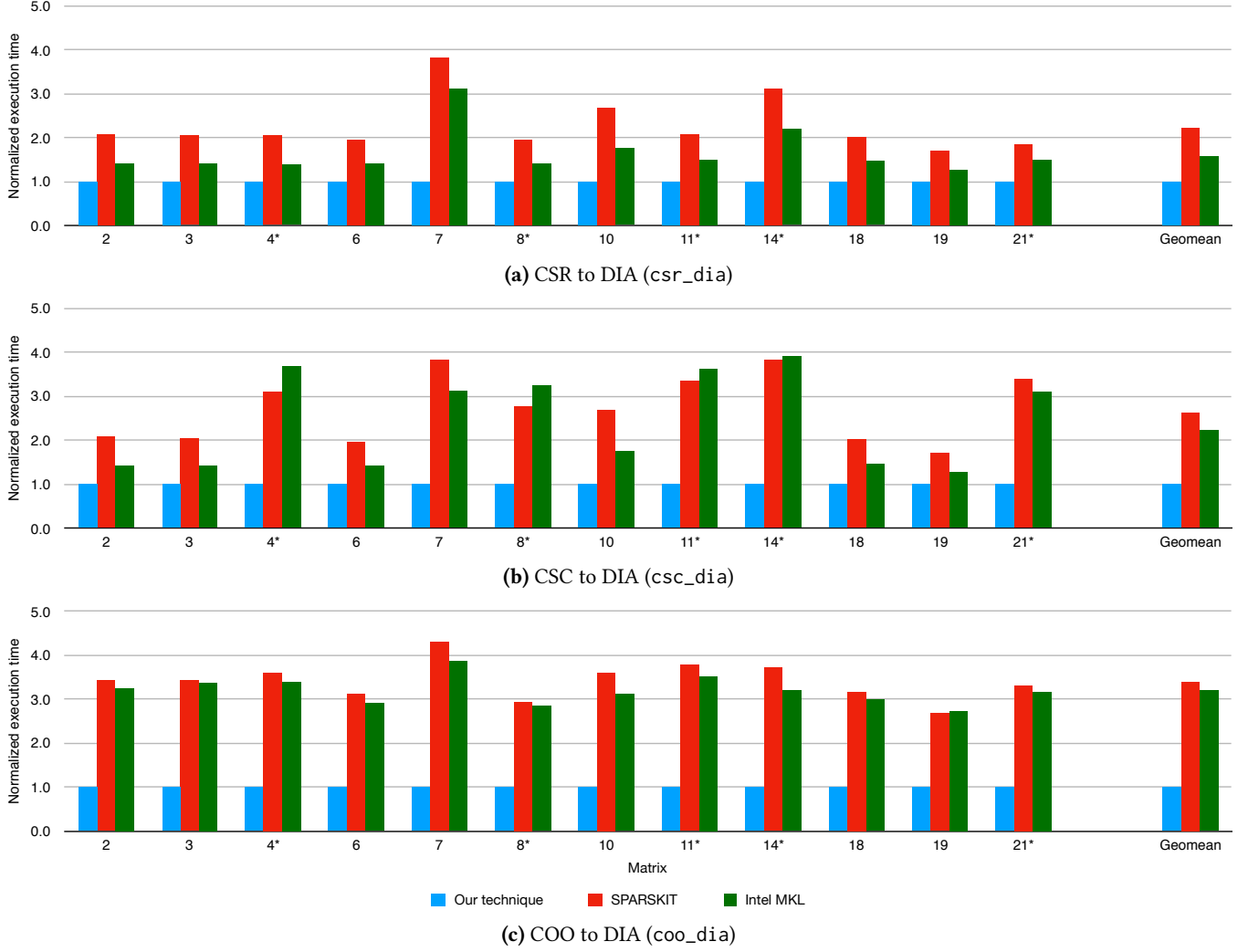


Figure 11. Normalized execution times of conversions to DIA, using code that our technique generates and other existing libraries. Results are normalized to that of our technique for each test matrix. Asterisks denote nonsymmetric matrices. For symmetric matrices, we cast CSC to DIA conversion as CSR to DIA conversion and report the same results shown in Figure 11a. We only show results for matrices that can be stored in DIA with at least 25% of stored values being nonzeros.

By expressing COO to CSR conversion in index notation as tensor assignment, the techniques of Kjolstad et al. and Chou et al. can also generate code that performs the conversion. As Figure 9 also shows though, our technique emits code to perform COO to CSR conversion that is 21.3 \times faster on average. The techniques of Kjolstad et al. and Chou et al. cannot reason about generating code that inserts nonzeros into CSR indices out of order. Thus, it must also sort the input before performing the actual conversion, incurring significant additional overhead. Furthermore, index notation cannot express conversions between formats that store nonzeros in non-lexicographic coordinate order. So without our extensions, taco cannot emit code to perform conversion end to end with structured formats like DIA or ELL.

8 Related Works

There exists a long line of works [5, 8, 9, 12, 19, 29–31, 40, 43, 48] on developing new sparse tensor formats to accelerate sparse matrix-vector multiplication (SpMV), sparse matrix-dense matrix multiplication (SpDM), matricized tensor times Khatri-Rao products (MTTKRP), and other sparse tensor algebra kernels. These formats organize nonzeros in disparate ways to reduce memory footprint, improve cache utilization, expose parallelization opportunities, and better exploit hardware capabilities such as SIMD vector units for performance. All the aforementioned works rely on hand-implemented routines for converting tensors from more common representations to their proposed formats. These routines are often as complex as the code to actually perform computations

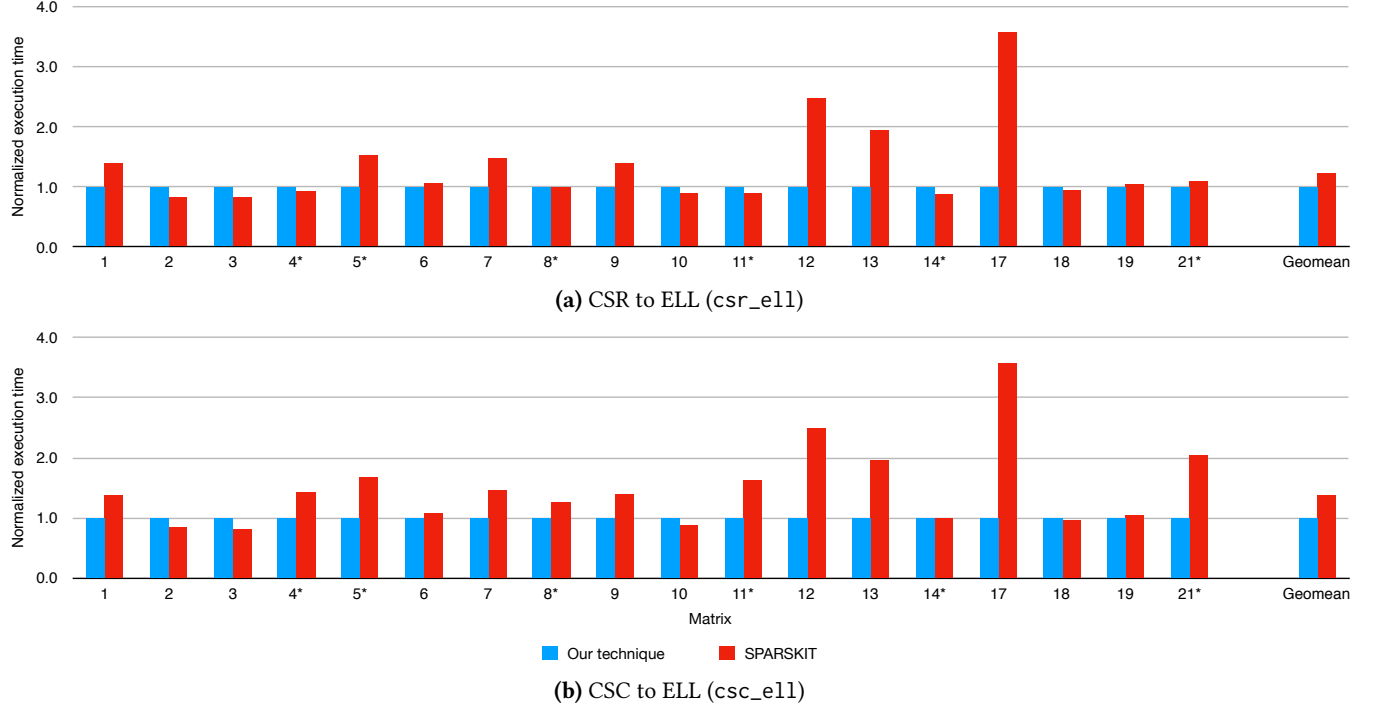


Figure 12. Normalized execution times of conversions to ELL, using code that our technique generates and other existing libraries. Results are normalized to that of our technique for each test matrix. Asterisks denote nonsymmetric matrices. For symmetric matrices, we cast CSC to ELL conversion as CSR to ELL conversion and report the same results shown in Figure 12a. We only show results for matrices that can be stored in ELL with at least 25% of stored values being nonzeros.

that the proposed formats are designed to accelerate. Additionally, many techniques [17, 18, 47] have been proposed for accelerating transpositions of CSR matrices, which is equivalent to converting matrices from CSR to CSC.

Existing sparse tensor and linear algebra compilers cannot generate efficient code to convert tensors between arbitrary, disparate formats. *taco* [14, 24, 25] can emit code to convert tensors between formats that store nonzeros in lexicographic coordinate order, but cannot generate complete conversion routines for structured formats like DIA and ELL. *taco* without our extensions also cannot emit code that computes and uses statistics about the input tensor to coordinate efficient assembly of the output tensor. *LL* [3, 4] is a functional language that lets user define sparse matrix formats as nestings of list and pairs that encode nonzeros in a dense matrix. From these specifications, the *LL* compiler can emit code that convert dense matrices to different sparse matrix formats, but not efficient code that directly convert between sparse matrix formats. *SIPR* [38], *CHiLL* [46], and techniques that Bik and Wijshoff [10, 11] proposed can all generate sparse linear algebra kernels that, as sub-operations, convert matrices between different formats. However, conversions in *SIPR*-generated code are performed by invoking hand-implemented operations that are hard-coded to specific source and target formats. The other techniques, meanwhile, only support a fixed

set of standard sparse matrix formats. *Bernoulli* [26, 27, 44] uses a black-box protocol that provides an abstract interface for describing how sparse matrices stored in different data structures can be efficiently accessed. However, the interface does not support assembly, so *Bernoulli* cannot generate code that constructs sparse matrix results.

There also exists a separate line of works [13, 22, 28, 33] on generating efficient code for query languages like SQL, which our attribute query language resembles. (Attribute queries are analogous to GROUP BY queries on a table that stores the coordinates of nonzeros.) In particular, *HorseIR* [13] lowers SQL queries to an array-based intermediate representation that is then optimized and compiled to efficient code. *Empty-Headed* [1], meanwhile, is a graph processing framework that generates efficient code to compute graph queries expressed in a Datalog-like language. Furthermore, our approach to optimizing attribute queries is reminiscent of query rewriting systems in certain relational database systems like *Starburst* [36, 37]. All these techniques are designed for queries that may perform complex joins and aggregate data of arbitrary types. By contrast, attribute queries are limited to aggregating (integer) coordinates. This lets our technique lower and optimize attribute queries in ways that would not be valid for aggregations over other types of data.

9 Conclusions

We have described a technique for generating sparse tensor conversion routines that efficiently convert tensors between a wide range of disparate formats. Our technique is extensible, and we have shown how even users can easily add support for new source and target formats by simply specifying how to construct and iterate over tensors in those new formats. By making it easy to work with the same data in multiple formats, each suited to a different stage of an application, our technique can greatly reduce the engineering effort needed to optimize sparse tensor algebra applications.

Acknowledgments

We thank Peter Ahrens, Rawn Henry, and Ziheng Wang for their helpful reviews and suggestions. This work was supported by the Application Driving Architectures (ADA) Research Center, a JUMP Center co-sponsored by SRC and DARPA; the Toyota Research Institute; the U.S. Department of Energy, Office of Science, Office of Advanced Scientific Computing Research; the National Science Foundation; and DARPA. Any opinions, findings, and conclusions or recommendations expressed in this material are those of the authors and do not necessarily reflect the views of the aforementioned funding agencies.

References

- [1] Christopher R. Aberger, Andrew Lamb, Susan Tu, Andres Nötzli, Kunle Olukotun, and Christopher Ré. 2017. EmptyHeaded: A Relational Engine for Graph Processing. *ACM Trans. Database Syst.* 42, 4, Article 20 (Oct. 2017), 44 pages. <https://doi.org/10.1145/3129246>
- [2] Animashree Anandkumar, Rong Ge, Daniel Hsu, Sham M. Kakade, and Matus Telgarsky. 2014. Tensor Decompositions for Learning Latent Variable Models. *J. Mach. Learn. Res.* 15, Article 1 (Jan. 2014), 60 pages.
- [3] Gilad Arnold. 2011. *Data-Parallel Language for Correct and Efficient Sparse Matrix Codes*. Ph.D. Dissertation. University of California, Berkeley.
- [4] Gilad Arnold, Johannes Hölzl, Ali Sinan Köksal, Rastislav Bodík, and Mooly Sagiv. 2010. Specifying and Verifying Sparse Matrix Codes. In *Proceedings of the 15th ACM SIGPLAN International Conference on Functional Programming (ICFP '10)*. ACM, New York, NY, USA, 249–260. <https://doi.org/10.1145/1863543.1863581>
- [5] Arash Ashari, Naser Sedaghati, John Eisenlohr, and P. Sadayappan. 2014. An Efficient Two-dimensional Blocking Strategy for Sparse Matrix-vector Multiplication on GPUs. In *Proceedings of the 28th ACM International Conference on Supercomputing (ICS '14)*. ACM, New York, NY, USA, 273–282. <https://doi.org/10.1145/2597652.2597678>
- [6] Brett W. Bader, Michael W. Berry, and Murray Browne. 2008. *Discussion Tracking in Enron Email Using PARAFAC*. Springer London, 147–163.
- [7] Brett W Bader and Tamara G Kolda. 2007. Efficient MATLAB computations with sparse and factored tensors. *SIAM Journal on Scientific Computing* 30, 1 (2007), 205–231.
- [8] M. Baskaran, B. Meister, N. Vasilache, and R. Lethin. 2012. Efficient and scalable computations with sparse tensors. In *2012 IEEE Conference on High Performance Extreme Computing*. 1–6. <https://doi.org/10.1109/HPEC.2012.6408676>
- [9] Nathan Bell and Michael Garland. 2009. Implementing Sparse Matrix-vector Multiplication on Throughput-oriented Processors. In *Proceedings of the Conference on High Performance Computing Networking, Storage and Analysis (SC '09)*. ACM, New York, NY, USA, Article 18, 11 pages. <https://doi.org/10.1145/1654059.1654078>
- [10] Aart JC Bik and Harry AG Wijshoff. 1993. Compilation techniques for sparse matrix computations. In *Proceedings of the 7th international conference on Supercomputing*. ACM, 416–424.
- [11] Aart JC Bik and Harry AG Wijshoff. 1994. On automatic data structure selection and code generation for sparse computations. In *Languages and Compilers for Parallel Computing*. Springer, 57–75.
- [12] Aydin Buluç, Jeremy T Fineman, Matteo Frigo, John R Gilbert, and Charles E Leiserson. 2009. Parallel sparse matrix-vector and matrix-transpose-vector multiplication using compressed sparse blocks. In *Proceedings of the twenty-first annual symposium on Parallelism in algorithms and architectures*. ACM, 233–244.
- [13] Hanfeng Chen, Joseph Vinish D'silva, Hongji Chen, Bettina Kemme, and Laurie Hendren. 2018. HorselR: Bringing Array Programming Languages Together with Database Query Processing. In *Proceedings of the 14th ACM SIGPLAN International Symposium on Dynamic Languages (DLS 2018)*. ACM, New York, NY, USA, 37–49. <https://doi.org/10.1145/3276945.3276951>
- [14] Stephen Chou, Fredrik Kjolstad, and Saman Amarasinghe. 2018. Format Abstraction for Sparse Tensor Algebra Compilers. *Proc. ACM Program. Lang.* 2, OOPSLA, Article 123 (Oct. 2018), 30 pages.
- [15] Timothy A. Davis and Yifan Hu. 2011. The University of Florida Sparse Matrix Collection. *ACM Trans. Math. Softw.* 38, 1, Article 1 (Dec. 2011).
- [16] Eduardo F. D'Azevedo, Mark R. Fahey, and Richard T. Mills. 2005. Vectorized Sparse Matrix Multiply for Compressed Row Storage Format. In *Proceedings of the 5th International Conference on Computational Science - Volume Part I (ICCS'05)*. Springer-Verlag, Berlin, Heidelberg, 99–106. https://doi.org/10.1007/11428831_13
- [17] Miguel A. Gonzalez-Mesa, Eladio D. Gutierrez, and Oscar Plata. 2013. Parallelizing the Sparse Matrix Transposition: Reducing the Programmer Effort Using Transactional Memory. *Procedia Computer Science* 18 (2013), 501 – 510. <https://doi.org/10.1016/j.procs.2013.05.214> 2013 International Conference on Computational Science.
- [18] Fred G. Gustavson. 1978. Two Fast Algorithms for Sparse Matrices: Multiplication and Permuted Transposition. *ACM Trans. Math. Softw.* 4, 3 (Sept. 1978), 250–269. <https://doi.org/10.1145/355791.355796>
- [19] Eun-jin Im and Katherine Yelick. 1998. Model-Based Memory Hierarchy Optimizations for Sparse Matrices. In *In Workshop on Profile and Feedback-Directed Compilation*.
- [20] Intel. 2012. *Intel math kernel library reference manual*. Technical Report. 630813-051US, 2012. <http://software.intel.com/sites/products/documentation/hpc/mkl/mklman/mklman.pdf>.
- [21] Yuanlin Jiang. 2007. *Techniques for Modeling Complex Reservoirs and Advanced Wells*. Ph.D. Dissertation. Stanford University.
- [22] Jun Rao, H. Pirahesh, C. Mohan, and G. Lohman. 2006. Compiled Query Execution Engine using JVM. In *22nd International Conference on Data Engineering (ICDE'06)*. 23–23. <https://doi.org/10.1109/ICDE.2006.40>
- [23] David R. Kincaid, Thomas C. Oppe, and David M. Young. 1989. *IT-PACKV 2D User's Guide*.
- [24] Fredrik Kjolstad, Peter Ahrens, Shoaib Kamil, and Saman Amarasinghe. 2019. Tensor Algebra Compilation with Workspaces. (2019), 180–192. <http://dl.acm.org/citation.cfm?id=3314872.3314894>
- [25] Fredrik Kjolstad, Shoaib Kamil, Stephen Chou, David Lugato, and Saman Amarasinghe. 2017. The Tensor Algebra Compiler. *Proc. ACM Program. Lang.* 1, OOPSLA, Article 77 (Oct. 2017), 29 pages. <https://doi.org/10.1145/3133901>
- [26] Vladimir Kotlyar. 1999. *Relational Algebraic Techniques for the Synthesis of Sparse Matrix Programs*. Ph.D. Dissertation. Cornell University.
- [27] Vladimir Kotlyar, Keshav Pingali, and Paul Stodghill. 1997. A relational approach to the compilation of sparse matrix programs. In *Euro-Par'97 Parallel Processing*. Springer, 318–327.
- [28] K. Krikellas, S. D. Viglas, and M. Cintra. 2010. Generating code for holistic query evaluation. In *2010 IEEE 26th International Conference*

- on Data Engineering (ICDE 2010). 613–624. <https://doi.org/10.1109/ICDE.2010.5447892>
- [29] Jiajia Li, Jimeng Sun, and Richard Vuduc. 2018. HiCOO: Hierarchical Storage of Sparse Tensors. In *Proceedings of the International Conference for High Performance Computing, Networking, Storage, and Analysis (SC '18)*. IEEE Press, Piscataway, NJ, USA, Article 19, 15 pages. <https://doi.org/10.1109/SC.2018.00022>
- [30] B. Liu, C. Wen, A. D. Sarwate, and M. M. Dehnavi. 2017. A Unified Optimization Approach for Sparse Tensor Operations on GPUs. In *2017 IEEE International Conference on Cluster Computing (CLUSTER)*. 47–57. <https://doi.org/10.1109/CLUSTER.2017.75>
- [31] Weifeng Liu and Brian Vinter. 2015. CSR5: An Efficient Storage Format for Cross-Platform Sparse Matrix-Vector Multiplication. In *Proceedings of the 29th ACM on International Conference on Supercomputing (ICS '15)*. ACM, New York, NY, USA, 339–350. <https://doi.org/10.1145/2751205.2751209>
- [32] Guy M Morton. 1966. *A computer oriented geodetic data base and a new technique in file sequencing*. Technical report.
- [33] Thomas Neumann. 2011. Efficiently Compiling Efficient Query Plans for Modern Hardware. *Proc. VLDB Endow.* 4, 9 (June 2011), 539–550. <https://doi.org/10.14778/2002938.2002940>
- [34] Jongsoo Park, Sheng Li, Wei Wen, Ping Tak Peter Tang, Hai Li, Yiran Chen, and Pradeep Dubey. 2016. Faster CNNs with Direct Sparse Convolutions and Guided Pruning. *arXiv:cs.CV/1608.01409*
- [35] Andrés Peratta and Viktor Popov. 2006. A new scheme for numerical modelling of flow and transport processes in 3D fractured porous media. *Advances in Water Resources* 29, 1 (2006), 42 – 61. <https://doi.org/10.1016/j.advwatres.2005.05.004>
- [36] Hamid Pirahesh, Joseph M. Hellerstein, and Waqar Hasan. 1992. Extensible/Rule Based Query Rewrite Optimization in Starburst. In *Proceedings of the 1992 ACM SIGMOD International Conference on Management of Data (SIGMOD '92)*. ACM, New York, NY, USA, 39–48. <https://doi.org/10.1145/130283.130294>
- [37] Hamid Pirahesh, T. Y. Cliff Leung, and Waqar Hasan. 1997. A Rule Engine for Query Transformation in Starburst and IBM DB2 C/S DBMS. In *Proceedings of the Thirteenth International Conference on Data Engineering (ICDE '97)*. IEEE Computer Society, Washington, DC, USA, 391–400. <http://dl.acm.org/citation.cfm?id=645482.653436>
- [38] William Pugh and Tatiana Shpeisman. 1999. SIPR: A new framework for generating efficient code for sparse matrix computations. In *Languages and Compilers for Parallel Computing*. Springer, 213–229.
- [39] Samyam Rajbhandari, Yuxiong He, Olatunji Ruwase, Michael Carbin, and Trishul Chilimbi. 2017. Optimizing CNNs on Multicores for Scalability, Performance and Goodput. In *Proceedings of the Twenty-Second International Conference on Architectural Support for Programming Languages and Operating Systems (ASPLOS '17)*. ACM, New York, NY, USA, 267–280. <https://doi.org/10.1145/3037697.3037745>
- [40] Youcef Saad. 1989. Krylov Subspace Methods on Supercomputers. *SIAM J. Sci. Stat. Comput.* 10, 6 (Nov. 1989), 1200–1232. <https://doi.org/10.1137/0910073>
- [41] Youcef Saad. 1994. SPARSKIT: a basic tool kit for sparse matrix computations - Version 2.
- [42] Yousef Saad. 2003. *Iterative methods for sparse linear systems*. SIAM.
- [43] Shaden Smith and George Karypis. 2015. Tensor-matrix products with a compressed sparse tensor. In *Proceedings of the 5th Workshop on Irregular Applications: Architectures and Algorithms*. ACM, 5.
- [44] Paul Stodghill. 1997. *A Relational Approach to the Automatic Generation of Sequential Sparse Matrix Codes*. Ph.D. Dissertation. Cornell University.
- [45] William F Tinney and John W Walker. 1967. Direct solutions of sparse network equations by optimally ordered triangular factorization. *Proc. IEEE* 55, 11 (1967), 1801–1809.
- [46] Anand Venkat, Mary Hall, and Michelle Strout. 2015. Loop and Data Transformations for Sparse Matrix Code. In *Proceedings of the 36th ACM SIGPLAN Conference on Programming Language Design and Implementation (PLDI 2015)*. 521–532.
- [47] Hao Wang, Weifeng Liu, Kaixi Hou, and Wu-chun Feng. 2016. Parallel Transposition of Sparse Data Structures. In *Proceedings of the 2016 International Conference on Supercomputing (ICS '16)*. Association for Computing Machinery, New York, NY, USA, Article Article 33, 13 pages. <https://doi.org/10.1145/2925426.2926291>
- [48] Biwei Xie, Jianfeng Zhan, Xu Liu, Wanling Gao, Zhen Jia, Xiwen He, and Lixin Zhang. 2018. CVR: Efficient Vectorization of SpMV on x86 Processors. In *Proceedings of the 2018 International Symposium on Code Generation and Optimization (CGO 2018)*. ACM, New York, NY, USA, 149–162. <https://doi.org/10.1145/3168818>